Experimental Animals
Exp. Anim. 74(2), 286–299, 2025

Original

Differential regulation of K^+-Cl^- cotransporter 2 (KCC2) and Na^+-K^+-Cl^- cotransporter 1 (NKCC1) expression by zolpidem in CA1 and CA3 hippocampal subregions of the lithium-pilocarpine status epilepticus rat model

Muhammad Zulfadhli OTHMAN[1)], Mohd Hamzah MOHD NASIR[2)], Wan Amir Nizam WAN AHMAD[3)], Jafri Malin ABDULLAH[1)] and Ahmad Tarmizi CHE HAS[1)]

[1)]*Department of Neurosciences, School of Medical Sciences, Universiti Sains Malaysia, Health Campus, Kubang Kerian, 16150 Kota Bharu, Kelantan, Malaysia*
[2)]*Department of Biotechnology, Kuliyyah of Science, International Islamic University Malaysia, Jalan Sultan Ahmad Shah, Bandar Indera Mahkota, 25200 Kuantan, Pahang, Malaysia*
[3)]*School of Health Sciences, Universiti Sains Malaysia, Health Campus, Kubang Kerian, 16150 Kota Bharu, Kelantan, Malaysia*

Abstract: Status epilepticus is linked to cognitive decline due to damage to the hippocampus, a key structure involved in cognition. The hippocampus's high vulnerability to epilepsy-related damage is the main reason for this impairment. Convulsive seizures, such as those observed in status epilepticus, can cause various hippocampal pathologies, including inflammation, abnormal neurogenesis, and neuronal death. Interestingly, substantial evidence points to the therapeutic potential of the sedative/hypnotic agent zolpidem for neurorehabilitation in brain injury patients, following the unexpected discovery of its paradoxical awakening effect. In this study, we successfully established an ideal lithium-pilocarpine rat model of status epilepticus, which displayed significant deficits in hippocampal-dependent learning and memory. The Morris water maze test was used to assess zolpidem's potential to improve learning and memory, as well as its impact on anxiety-like behavior and motor function. Immunohistochemical staining and fluorescence analysis were used to examine the effect of zolpidem on K^+-Cl^- cotransporter 2 (KCC2) and Na^+-K^+-Cl^- cotransporter 1 (NKCC1) protein expression in the hippocampal CA1 and CA3. Our findings showed that zolpidem did not improve learning and memory in status epilepticus rats. Additionally, its sedative/hypnotic effects were not apparent in the status epilepticus condition. However, immunohistochemical results revealed that zolpidem significantly restored altered NKCC1 levels in the CA1 and CA3 to levels similar to those seen in normal rats. These findings suggest that zolpidem may contribute to molecular restoration, particularly through its impact on NKCC1 protein expression in the hippocampus, which is crucial for proper inhibitory neurotransmission in the brain.

Key words: hippocampus, K^+-Cl^- cotransporter 2 (KCC2), Na^+-K^+-Cl^- cotransporter 1 (NKCC1), status epilepticus, zolpidem

Introduction

Status epilepticus (SE) is associated with cognitive decline due to the damage to several brain areas, including the hippocampus. The hippocampus is a brain region linked to cognitive functions, such as learning and memory [1–5]. The harmful effects of SE on the hippocampus can be recognized by various neuropathological changes, such as neuronal loss, astrogliosis, neuroinflammation, abnormal neurogenesis, and synap-

(Received 17 September 2024 / Accepted 25 December 2024 / Published online in J-STAGE 9 January 2025)
Corresponding author: A.T. Che Has. email ahmadtarmizi@usm.my
Supplementary Figures: refer to J-STAGE: https://www.jstage.jst.go.jp/browse/expanim

tic reorganization [3, 6, 7]. Increasing evidence has highlighted the potential therapeutic benefits of the sedative and hypnotic agent zolpidem in facilitating brain injury recovery following the serendipitous discovery of its paradoxical effects in 2000 [8, 9]. Several studies have consistently reported the ability of zolpidem to recover various physiological functions, such as brain functional connectivity, cerebral blood flow, activation of dormant brain areas, and enhancement of behavioral impairments and cognitive functions [9–13].

Zolpidem acts on γ-aminobutyric acid type-A receptors (GABAARs) by modulating their functions in the presence of GABA. Under normal physiological conditions, the activation of GABAAR allows Cl^- to flow into the neuron along its electrochemical gradient due to the higher concentration of Cl^- in the extracellular space than in the intracellular region, leading to neuronal hyperpolarization. The Cl^- electrochemical gradient is primarily sustained by the combined action of cation-chloride cotransporters (CCCs), specifically Na^+-K^+-Cl^- cotransporter 1 (NKCC1) and K^+-Cl^- cotransporter 2 (KCC2), which respectively bring Cl^- into and remove Cl^- from the cell [14, 15]. KCC2 is predominantly expressed in most mature central neurons, whereas NKCC1 is expressed in both immature and diseased central neurons [16]. KCC2 helps expel Cl^- from neurons, reducing the intracellular Cl^- concentration and promoting Cl^- influx when GABAARs are activated. However, under certain conditions, such as epilepsy, KCC2 is downregulated and NKCC1 is upregulated, reversing the Cl^- electrochemical gradient and resulting in a higher Cl^- concentration inside the neurons than in the extracellular space [15].

Consequently, the activation of GABAARs leads to a net outflow of Cl^-, which depolarizes neurons and shifts the role of GABAARs from inhibitory to excitatory. GABAAR-mediated depolarization can be modulated or enhanced by various receptor-modulating drugs, including zolpidem. This hypothesis may explain the paradoxical effects of zolpidem in promoting awakening and behavioral improvement, particularly in cases of brain injury. Ben-Ari suggested that the zolpidem-mediated awakening effects in brain injury may result from a shift in inhibitory GABAergic transmission to excitatory neurons, which is primarily determined by the intracellular Cl^- concentration and the synergistic roles of NKCC1 and KCC2 [17]. Despite this promising hypothesis, limited knowledge is available about the underlying mechanisms and full extent of the effects of zolpidem *in vivo*. Testing this hypothesis in preclinical animal models presents significant challenges, as a comprehensive understanding of the drug's effects on behavior, cellular physiology, and molecular signaling requires diverse experimental approaches. Nevertheless, animal models offer a powerful platform for investigating underlying mechanisms and testing interventions that are impractical in clinical settings, providing critical insights into the paradoxical effects of zolpidem. Consequently, additional research is essential to completely clarify the mechanisms underlying this effect on brain injury and assess the therapeutic potential of the drug.

In this study, a lithium-pilocarpine rat model of status epilepticus was developed using lithium, an optimal dose of pilocarpine, xylazine, and a drug cocktail containing diazepam and MK-801. The Morris water maze (MWM) test was employed to assess zolpidem's potential to enhance learning and memory, along with its effects on anxiety-like behavior and motor function. Quantitative histological analysis was conducted to evaluate cell layer thickness and absolute cell number in the principal cell layers of the CA1 and CA3 hippocampal regions in rats with lithium-pilocarpine-induced status epilepticus, using hematoxylin and eosin staining. Additionally, immunohistochemical staining and fluorescence quantification were performed to investigate zolpidem's impact on KCC2 and NKCC1 protein expression in these regions.

Materials and Methods

Animal quarantine and acclimatization

The experiments were conducted in accordance with the institutional guidelines and were approved by the Animal Ethics Committee of Universiti Sains Malaysia [USM/IACUC/2021/(127)(1120)]. Eight-week-old male Sprague-Dawley rats, weighing 250 to 300 g, were used and housed in a controlled environment at room temperature with a standard 12:12 light/dark cycle, with food pellets and water available *ad libitum*. The study spanned 26 days, starting with lithium chloride (LiCl) injection on Day 1 and ending with the preparation of brain samples on Day 26.

Developing the lithium-pilocarpine model of epilepsy

All rats were administered an intraperitoneal (i.p.) injection of LiCl (127 mg/kg) (MP Biomedicals, Santa Ana, CA, USA), 16–24 h prior before pilocarpine hydrochloride administration (Day 1). On the following day (Day 2), pilocarpine (MP Biomedicals) was administered intraperitoneally every 30 min at doses of 20 + 10 + 10 + 10 mg/kg, up to a maximum cumulative dose of 50 mg/kg until status epilepticus (SE) was induced [18–20]. SE was characterized by continuous limbic seizures lasting for at least 30 min, reaching stage 4 or 5 on the Racine scale [21, 22]. Only rats that developed

sustained SE were included in further experiments. To terminate SE, rats were initially injected with 2.5 mg/kg xylazine (Ilium Xylazil-100; Troy Laboratories Pty Ltd., NSW, Australia). After remaining in the xylazine-modified state for one hour, they were given a drug cocktail of 2.5 mg/kg of diazepam (LGC Standards Ltd., Teddington, UK) and 0.1 mg/kg of MK-801 (Abcam Ltd., Cambridge, UK) intraperitoneally to completely stop SE [23]. The rats were allowed to recover during the post-seizure period (Day 3 to 19).

Morris water maze

Rats underwent the MWM test to evaluate the effect of zolpidem on spatial learning and memory retrieval [24, 25]. The MWM protocol for the assessment of spatial memory retrieval was adapted from [26]. In addition, the effects of zolpidem on anxiety-like behavior and motor function were assessed. Anxiety-like behavior was measured by the time spent and path length at the periphery of the pool [27, 28], whereas motor function was assessed using average swimming speed [29]. The rats were divided into four treatment groups: $Control_{Vehicle}$, $Control_{Zolpidem}$, $SE_{Vehicle}$, and $SE_{Zolpidem}$. In the MWM task, the rats underwent a 60 s habituation day (Day 20), followed by four days of training (Day 21 to 24) with four 60 s trials each day and a 60 s probe trial on the final day (Day 25) [30, 31]. The water was contained in a black circular pool (150 cm diameter, 64 cm deep), maintained at 25 ± 1°C. An invisible, submerged escape platform (10 cm diameter, 44 cm high) was placed in the center of the southeast quadrant during the training sessions and removed during habituation and probe trials. Throughout the procedure, rats were released facing the pool wall.

During habituation, rats were allowed to swim freely in the pool for 60 s. During the training period, the time required by each rat to reach the platform was recorded. The rats that failed to find the platform were gently guided onto it by the experimenter and allowed to stay there for 10 s before being transferred to a quarantine cage for drying. During the probe trial, the rats were administered zolpidem (2.5 mg/kg, i.p.) (LGC Standards Ltd.) or vehicle (0.9% saline) 30 min before the trial began. The zolpidem dose was chosen based on dose-response curves indicating a 50% effective dose (ED50) of zolpidem for impairing locomotor behavior in mice and rats, ranging from 1.0 to 2.5 mg/kg [32, 33]. The rats were then released from the northeast. The time spent in the target southeast quadrant was video-recorded and analyzed using a behavioral tracking software (Smart© Version 3.0.05, Panlab, Barcelona, Spain). Additionally, the time spent and path length at the periphery, along with the mean speed, were analyzed to assess anxiety-like behaviors and motor function. For analysis, the pool was divided into eight zones (northeast, southeast, southwest, and northwest), with each quadrant subdivided into internal and external zones [27].

Brain sample preparation

On Day 26, the rats were euthanized using CO_2 and subjected to whole-body perfusion with 0.9% saline, followed by 4% paraformaldehyde (PFA) (Sigma-Aldrich, St. Louis, MO, USA). The brains were fixed in 10% neutral-buffered formalin (NBF) at 4°C for 48 h and then placed in 70% ethanol. The coronal gross was confirmed by visualization of the entire dorsal hippocampus (Bregma −2.5 and −4.5 mm) according to [34]. The tissue sections were fixed, dehydrated, cleared, and embedded in paraffin. Subsequently, the tissues were embedded in paraffin and sectioned at a thickness of 5 μm.

Histology

Tissue sections were dewaxed and rehydrated prior to hematoxylin and eosin (H&E) staining, which was carried out using hematoxylin (Leica Biosystems, Nussloch, Germany) and eosin (Leica Biosystems). The stained sections were mounted and cover-slipped with DPX (Merck, Darmstadt, Germany).

Immunohistochemistry

Tissues were also subjected to sequential double-fluorescence labeling of KCC2 and NKCC1 proteins as performed by [35] with some optimizations. They were first dewaxed with xylene and then gradually rehydrated with decreasing concentrations of ethanol. Heat-induced antigen retrieval (HIAR) was performed using a citrate-based antigen retrieval solution (pH 6.0) antigen retrieval solution (Sigma-Aldrich). The tissues were blocked with 3% normal goat serum (NGS) (Sigma-Aldrich) and normal donkey serum (NDS) (Sigma-Aldrich). Subsequently, the tissues were incubated with an anti-KCC2 rabbit primary antibody overnight at 4°C (Abcam Ltd.). The following day, the tissues were incubated with goat anti-rabbit IgG secondary antibody (Thermo Fisher Scientific Inc.). After washing with PBS, the tissues were stained with NKCC1 staining. They were then incubated with an anti-NKCC1 goat primary antibody (Abcam Ltd.) overnight at 4°C, followed by incubation with a donkey anti-goat IgG secondary antibody (ThermoFisher Scientific Inc.). Finally, the tissues were washed with PBS and mounted with Fluoroshield™ containing 4',6-diamidino-2-phenylindole (DAPI) before cover-slipping.

Image acquisition

Microscopic histological and fluorescence images were acquired using a microscope (BX41, Olympus Corp., Tokyo, Japan), synchronized with the Olympus cellSens imaging software (cellSens2.2_RU_01, Olympus Corp.). For fluorescence, excitation at different fluorophore wavelengths was achieved using a mercury bulb burner (U-RFL-T, Olympus Corp.), set to 358 nm (blue), 488 nm (green), and 594 nm (red). The exposure time for image acquisition was set to 500 ms for both the red and green channels. Hematoxylin and DAPI nuclear staining were used to identify the hippocampal regions of interest (ROIs), specifically CA1 and CA3.

Microscopic quantitative analysis

Microscopic analyses of the CA1 and CA3 hippocampal subregions were conducted using ImageJ software (ImageJ 1.53c, National Institute of Health, Bethesda, MD, USA) for both histology and fluorescence quantification. Structures were identified according to standard anatomical criteria [34, 36]. For H&E staining, the thickness of the structure and absolute cell count within the CA1 and CA3 pyramidal cell layers (PCL) were measured according to [37]. Within each sub-region, three random regions of interest (ROIs) (0.253 mm^2 per ROI) were selected for cell number quantification. For fluorescence quantification, three random ROIs were chosen (25,515 μm^2). Background subtraction, image brightness, and contrast thresholds were set and standardized throughout the experiment. The raw integrated fluorescence density was evaluated. The fluorescence intensities of these ROIs were averaged to produce a single mean intensity value representing the intensity within the structure. The blue, red, and green channels were subsequently merged using ImageJ and Adobe Photoshop 2020 (version 21.1.3, Adobe Systems Software, Adobe Inc., San Jose, CA, USA) software to form a composite image.

Statistical analysis

Statistical analyses for the MWM and immunofluorescence studies were performed using GraphPad Prism9 (Version 9.0.1, GraphPad Software Inc., CA, USA). All datasets were tested for Gaussian distribution using the Shapiro-Wilk normality test prior to parametric analysis. An unpaired *t*-test was used to compare two groups. For comparisons involving three or more groups, ordinary one-way ANOVA was used, with Tukey's post-hoc analysis for multiple comparisons. For the four-day MWM training data comparison, a repeated two-way ANOVA was used with Tukey's post-hoc multiple comparisons. All data are plotted as mean values, with error bars representing the standard deviation. The significance level was set at $P<0.05$.

Results

Model development: Pilocarpine dose optimization and cocktail administration

Pilocarpine dose optimization is important for consistent seizure behavior, which is represented by the manifestation of continuous SE. In this study, we used dose optimization strategies. This involved limiting the cumulative ceiling dose and number of injections for each rat. We effectively induced SE in 27 rats with 21 (78%) of them successfully developed SE, characterized by the exhibition of ≥stage IV according to Racine Scale. The 21 rats which developed SE were grouped in the SE_{SIV-SV} group meanwhile another six unsuccesful SE induction were grouped in the $noSE_{SI-SIII}$ group. Animals exhibiting SE morbidity are predisposed to high mortality rates [38]. Therefore, xylazine and a cocktail containing diazepam and MK-801 were used in this study [23]. Drug intervention strategies are summarized in (Table 1).

Memory acquisition during training session

We first examined memory acquisition between the different treatment groups using a repeated two-way ANOVA to analyze the significant differences between treatments and days of training for all groups. The analysis revealed a significant difference in the latency to reach the platform between the different treatment groups throughout the four-days training period ($P<0.0001$). We further investigated the significant differences between

Table 1. Morbidity and mortality rates from the model development

Experiments	Experiment Design and Outcomes
Fractionation of pilocarpine doses	Pilocarpine rats received 20 + 10 + 10 + 10 mg/kg. Total dose = 50 mg/kg (maximum 4 injections).
Morbidity rate	Rats that developed SE = 21/27 (78 %)
Application of xylazine and drug cocktail to terminate SE	Termination with 2.5 mg/kg of xylazine 30 minutes after the SE, followed by systemic administration of drug cocktail containing (2.5 mg/kg diazepam and 0.1 mg/kg MK-801) within 1 hour after the xylazine intervention.
Mortality rate	Rats that died = 6/27 (22 %)

the different treatment groups for each day of the four-days training period using Tukey's post-hoc multiple comparison test. We found that, even starting from Day 1 of the training session, $SE_{SIV\text{-}SV}$ rats (58.96 ± 2.55 s) exhibited significantly impaired spatial learning as compared to control rats [Day 1 (47.03 ± 8.67 s, $P<0.05$)] (Fig. 1, Top). The learning and memory impairment aggravated throughout the remaining three days, from which the exhibition of significantly longer time taken to reach the platform was observed for the $SE_{SIV\text{-}SV}$ [Day 2 (57.29 ± 6.63 s), Day 3 (54.71 ± 6.58 s) and Day 4 (52.14 ± 5.54 s)] as compared to Control group [Day 2 (30.54 ± 11.97 s, $P<0.01$), Day 3 (10.93 ± 4.44 s, $P<0.01$) and Day 4 (6.64 ± 1.98 s, $P<0.0001$)] (Fig. 1, Top). In addition, no significant difference was noted between days 1 and 4 within the $SE_{SIV\text{-}SV}$ group, indicating that the rats were unable to learn spatial navigation.

However, possible spatial learning and memory deficits manifested by $noSE_{SI\text{-}SIII}$ rats have not yet been reported in other studies and remain elusive; therefore, we attempted to investigate this ambiguity. Comparatively, only during Day 3 and Day 4 the $noSE_{SI\text{-}SIII}$ rats [Day 3 (37.00 ± 14.94 s) and Day 4 (27.00 ± 14.56 s)] (Fig. 1, Top) revealed significantly shorter time latency as compared to their $SE_{SIV\text{-}SV}$ littermates ($P<0.05$). No significant difference was reported between the two groups throughout the first two days of training. This may indicate that the $noSE_{SI\text{-}SIII}$ rats showed gradual improvement in spatial learning and memory acquisition (only occurred starting from Day 3 and not as the $SE_{SIV\text{-}SV}$ rats), reflecting the considerable exhibition of spared spatial cognitive function in the $noSE_{SI\text{-}SIII}$ rats. The spared cognitive function displayed in the $noSE_{SI\text{-}SIII}$ rats may be further indicated by the non-significant difference in time latency between $noSE_{SI\text{-}SIII}$ rats and control rats for the first three consecutive days, but not on the final day, when $noSE_{SI\text{-}SIII}$ rats indicated a significantly longer time to reach the platform compared to their control littermates ($P<0.05$). Therefore, combining these two points, significant difference exhibited at Day 3 and 4 between $noSE_{SI\text{-}SIII}$ and $SE_{SIV\text{-}SV}$, and the exhibition of spared cognitive function in $noSE_{SI\text{-}SIII}$ rats, these may corroborate in term of cognitive function of why injury exhibited by this group may not be reliable in mimicking the model, and are widely excluded in most experiments.

Effect of acute zolpidem administration on the memory retrieval in the normal and SE rats

Next, we assessed the effect of zolpidem on the retrieval of spatial memory (quantified as the percentage of time spent in the target quadrant) in normal and SE rats. In addition, using other paradigms of the water

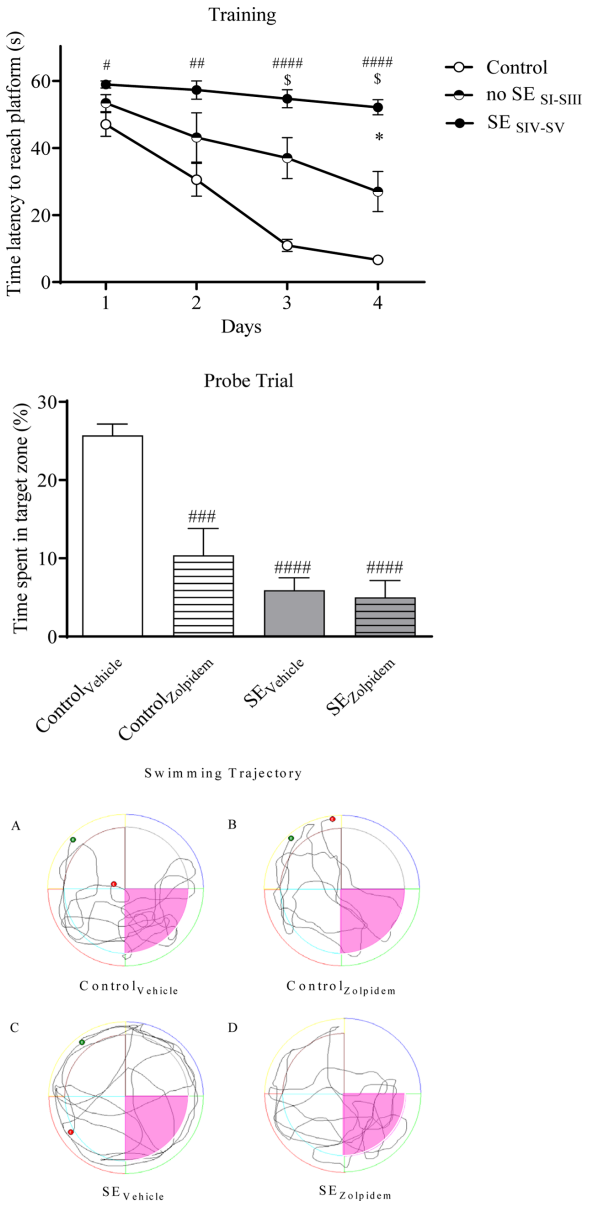

Fig. 1. Evaluation of long-term spatial memory in Morris water maze (MWM) over the 4-day training period (Top). Spatial memory performance was assessed by comparing the daily time latency (s) for Control, $noSE_{SI\text{-}SIII}$ and $SE_{SIV\text{-}V}$ rats to reach the escape platform. A two-way repeated measures ANOVA was used to assess the effects of group and day of training on latency. Statistical analysis annotations: $^{\#}P<0.05$, $^{\#\#}P<0.01$ and $^{\#\#\#\#}P<0.0001$ for comparisons between $SE_{SIV\text{-}SV}$ and Control. $^{\$}P<0.05$ for $SE_{SIV\text{-}SV}$ versus $noSE_{SI\text{-}SIII}$. $^{*}P<0.05$ for $noSE_{SI\text{-}SIII}$ versus Control. Number of animals used for each group=6. Effect of zolpidem on long-term spatial memory during probe trial in the MWM (Middle). One-way ANOVA was used to assess the effects of group ($Control_{Vehicle}$, $Control_{Zolpidem}$, $SE_{Vehicle}$, $SE_{Zolpidem}$). Percentage of time spent (%) in the target quadrant southeast. Statistical analysis annotations: $^{\#\#\#}P<0.001$ and $^{\#\#\#\#}P<0.0001$ versus $Control_{Vehicle}$. Number of animals used for each group=6. Effect of zolpidem on animals' swimming trajectories in the target quadrant during the MWM probe trial in (A) $Control_{Vehicle}$, (B) $Control_{Zolpidem}$, (C) $SE_{Vehicle}$ and (D) $SE_{Zolpidem}$ (Below). Swimming trajectories of the animals were tracked to quantify and analyse the % of time spent in the target quadrant, shaded in pink.

maze, including swimming speed in the maze and path length in the peripheral zone, we quantified the effects of zolpidem on motor function and anxiety. To assess the effect of zolpidem on retrieval memory in normal and SE rats, the time spent (%) in the south-east target quadrant (shaded pink) was used. A significant difference (P<0.0001) in the time spent in the target quadrant was observed between the treatment groups. Significant reduction of time spent in the target quadrant of the $Control_{Zolpidem}$ (10.39 ± 8.38%) as compared to the vehicle-treated normal rats (25.70 ± 3.58%, P<0.001), however, no significant difference was observed between the zolpidem-treated (5.00 ± 5.29%) and vehicle-treated (5.92 ± 3.93%) of the SE rats. $SE_{Vehicle}$ and $SE_{Zolpidem}$ rats showed a significant reduction in the time spent in the target quadrant compared to the $Control_{Vehicle}$ (P<0.0001) (Fig. 1, Middle). The negative memory effect of zolpidem under normal conditions was visualized by the impairment of the rats' search strategy compared to non-zolpidem-treated animals. The search strategies of zolpidem- and vehicle-treated SE animals were not profoundly different, as they exhibited similar patterns of impaired search trajectories (Fig. 1, Below). In this case, zolpidem did not enhance the memory retrieval process in the SE rats.

Effect of acute zolpidem administration on the anxiety-like behaviour, and motor function in the normal and SE rats

To assess the effect of zolpidem on anxiety-like behavior in the normal and SE groups, the path length (m) paradigm in the peripheral zone, shaded blue, was used. One-way ANOVA revealed a significant difference (P<0.001) in path length in the peripheral zone between the treatment groups. No significant difference of path length in the peripheral zone was observed between the vehicle-treated (4.83 ± 1.92 m) and zolpidem-treated (4.08 ± 1.43 m) in the normal rats (Fig. 2, Top; Left). The swimming trajectory of zolpidem-treated rats showed no notable difference in the peripheral swimming pattern and was indistinguishable from that observed in vehicle-treated rats (Fig. 2, Below). This reflects the weak anxiolytic effects of zolpidem under normal conditions. In addition, no significant difference was observed between the vehicle and zolpidem treatments in SE rats. Moreover, based on the swimming trajectory, zolpidem treatment in SE rats did not result in a different peripheral swimming pattern compared to vehicle-treated rats (Fig. 2, Below). This shows that the insignificant anxiolytic effect of zolpidem was retained in the SE condition, similar to that observed under normal conditions. Both vehicle- and zolpidem-treated SE rats exhibited a significant increase in path length in the peripheral zone compared with the $Control_{Vehicle}$ (P<0.01) and $Control_{Zolpidem}$ (P<0.01).

To assess the effect of zolpidem on motor function between the groups, mean speed (ms^{-1}) in the water maze was used. Zolpidem (0.287 ± 0.072 ms^{-1}) significantly impaired the motor function in normal rats (unpaired t-test; 0.37 ± 0.026 ms^{-1}, t=2.765, df=10, P<0.05), however, not in the SE rats ($SE_{Vehicle}$=0.420 ± 0.060 ms^{-1} and $SE_{Zolpidem}$=0.393 ± 0.092 ms^{-1}, t=0.5917, df=10; unpaired t-test) (Fig. 2, Top; Right). This highlights the sedative and hypnotic effects of zolpidem in normal rats, which are reflected in the presence of motor impairment in zolpidem-treated animals. However, zolpidem-mediated sedative and hypnotic effects were not observed in SE rats, which may indicate that zolpidem may not act as a sedative or hypnotic in brain injury conditions.

Histopathological studies in CA1 and CA3 hippocampal subregions of the zolpidem treated SE rats

Ordinary one-way ANOVA showed significant differences in mean thickness of the CA1 PCL of the various treatment groups (P<0.0001) (Fig. 3, Left). Tukey's post-hoc multiple comparison analysis revealed significant reduction in CA1 PCL mean thickness of the $SE_{Vehicle}$ (23.11 ± 4.783 μm, P<0.0001) and $SE_{Zolpidem}$ (24.92 ± 2.717 μm, P<0.0001) in comparison to $Control_{Vehicle}$ (42.85 ± 4.909 μm) and $Control_{Zolpidem}$ groups (43.63 ± 4.909 μm). Meanwhile, a significant differences in mean thickness of the CA3 PCL of the various treatment groups were observed (P<0.0001) (Fig. 3, Right). The $SE_{Vehicle}$ (40.80 ± 5.755 μm, P<0.0001) and $SE_{Zolpidem}$ (38.54 ± 3.814 μm, P<0.0001) groups showed a significant reduction in mean thickness compared to the $Control_{Vehicle}$ (62.46 ± 6.177 μm) and $Control_{Zolpidem}$ groups (65.45 ± 2.469 μm).

Regarding the absolute cell count, one-way ANOVA also showed significant differences in both CA1 and CA3 PCL between treatment groups (P<0.0001) (Fig. 4). Significant reductions in absolute cell number were found in the $SE_{Vehicle}$ (34.60 ± 3.627, P<0.0001) and $SE_{Zolpidem}$ (35.50 ± 3.646, P<0.0001) groups relative to the $Control_{Vehicle}$ (57.06 ± 2.797) and $Control_{Zolpidem}$ groups (58.00 ± 3.425). Likewise, the $SE_{Vehicle}$ (22.90 ± 1.853, P<0.0001) and $SE_{Zolpidem}$ (20.33 ± 2.102, P<0.0001) groups exhibited significant reductions in absolute cell number in the CA3 PCL compared to the $Control_{Vehicle}$ (42.03 ± 3.529) and $Control_{Zolpidem}$ groups (44.17 ± 4.284).

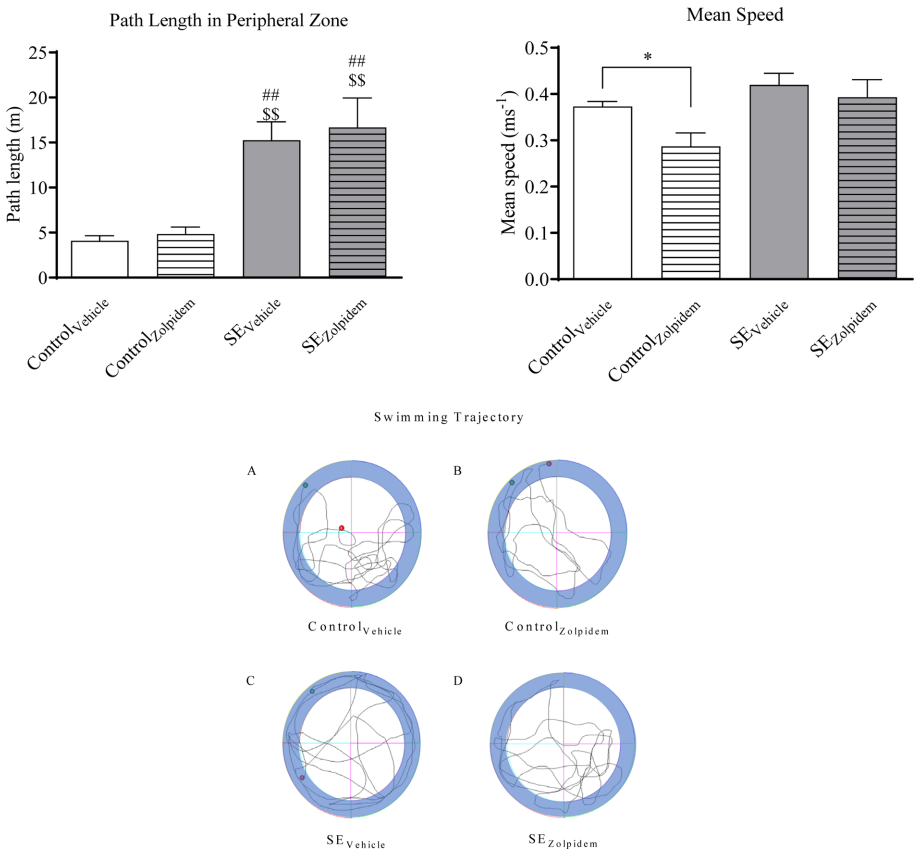

Fig. 2. Effect of zolpidem on the animal thigmotactic behaviour during the probe trial in the MWM (Top, Left). One-way ANOVA was used to assess the effects of group ($Control_{Vehicle}$, $Control_{Zolpidem,}$ $SE_{Vehicle}$, $SE_{Zolpidem}$). The evaluation was quantified by path length (m) in the peripheral zone. Statistical analysis annotations: $^{\#\#}P<0.01$ versus $Control_{Vehicle}$ and $^{\$\$}P<0.01$ versus $Control_{Zolpidem}$. Number of animals used for each group=6. Effect of zolpidem on the motor function mean speed (ms^{-1}) in the MWM test (Top, Right). Unpaired *t*-test was used to assess the effects of group (between $Control_{Vehicle}$ and $Control_{Zolpidem;}$ as well as between $SE_{Vehicle}$ and $SE_{Zolpidem}$). Statistical analysis annotations: $^{*}P<0.05$ and non-significant (n.s.) $P>0.05$. Number of animals used for each group=6. Effect of zolpidem on animals' thigmotactic swimming trajectories during the MWM probe trial in (A) $Control_{Vehicle}$, (B) $Control_{Zolpidem}$, (C) $SE_{Vehicle}$ and (D) $SE_{Zolpidem}$ (Below). Swimming trajectories of the animals were tracked to quantify and analyse the% of time allocation in the peripheral zone, shaded in blue.

Immunofluorescence studies: Expression of KCC2 and NKCC1 in CA1 and CA3 hippocampal subregions of the zolpidem treated SE rats

Ordinary one-way ANOVA showed significant difference in KCC2 expression in the CA1 PCL between the various treatment groups ($P<0.001$) (Fig. 5). We observed significant reduction the KCC2 expression in the $SE_{Vehicle}$ ($7.907 \times 10^7 \pm 4.582 \times 10^7$a. u.) in comparison to $Control_{Vehicle}$ ($1.604 \times 10^8 \pm 3.137 \times 10^7$a. u., $P<0.001$). CA1 PCL NKCC1 protein expression was significantly different between the protein expression between groups ($P<0.0001$). We observed significant increase of the raw integrated density of NKCC1 protein in the $SE_{Vehicle}$ ($1.175 \times 10^8 \pm 3.885 \times 10^7$a. u.) in comparison to $Control_{Vehicle}$ ($5.812 \times 10^7 \pm 2.552 \times 10^7$a. u., $P<0.001$). Additionally, we reported that $SE_{Zolpidem}$ (6.872×10^7–3.960×10^7a. u.) exhibited a significant decrease in NKCC1 expression compared to the $SE_{Vehicle}$ ($P<0.01$).

Ordinary one-way ANOVA showed significant differences in KCC2 protein expression in the CA3 PCL of the various treatment groups ($P<0.0001$) (Fig. 6). Multiple comparison analysis revealed significant reduction of the KCC2 expression in the CA3 PCL of the $SE_{Vehicle}$ ($8.228 \times 10^7 \pm 4.341 \times 10^7$a. u.) in comparison to $Control_{Vehicle}$ ($1.580 \times 10^8 \pm 1.469 \times 10^7$a. u., $P<0.001$). Moreover, $SE_{Zolpidem}$ ($9.208 \times 10^7 \pm 4.126 \times 10^7$a. u.) exhibited significantly decreased KCC2 protein expression compared to the $Control_{Vehicle}$ ($P<0.001$) and also to $Control_{Zolpidem}$ ($P<0.01$). We noted a significant difference in NKCC1 expression in CA3 cells ($P<0.0001$). We observed significant increase of the NKCC1 expression in the $SE_{Vehicle}$ ($1.227 \times 10^8 \pm 3.245 \times 10^7$a. u.) in

 doi: 10.1538/expanim.24-0120

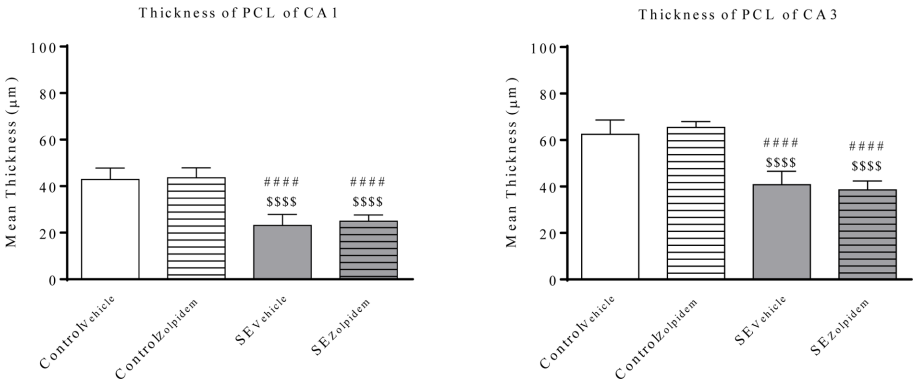

Fig. 3. Evaluation of mean structure thickness of pyramidal cell layer or PCL of the hippocampal CA1 (quantified in μm) (Left). One-way ANOVA was used to evaluate the thickness of PCL in CA1 ($Control_{Vehicle}$, $Control_{Zolpidem}$, $SE_{Vehicle}$, $SE_{Zolpidem}$). Significant differences were annotated as follows: $^{\#\#\#\#}P<0.0001$ versus $Control_{Vehicle}$, $^{\$\$\$\$}P<0.0001$ versus $Control_{Zolpidem}$. Number of animals used for each group=4–6. Evaluation of mean structure thickness of PCL of the hippocampal CA3 (quantified in μm) (Right). One-way ANOVA was used to evaluate the thickness of PCL in CA3 ($Control_{Vehicle}$, $Control_{Zolpidem}$, $SE_{Vehicle}$, $SE_{Zolpidem}$). Significant differences were annotated as follows: $^{\#\#\#\#}P<0.0001$ versus $Control_{Vehicle}$, $^{\$\$\$\$}P<0.0001$ versus $Control_{Zolpidem}$. Number of animals used for each group=4–6.

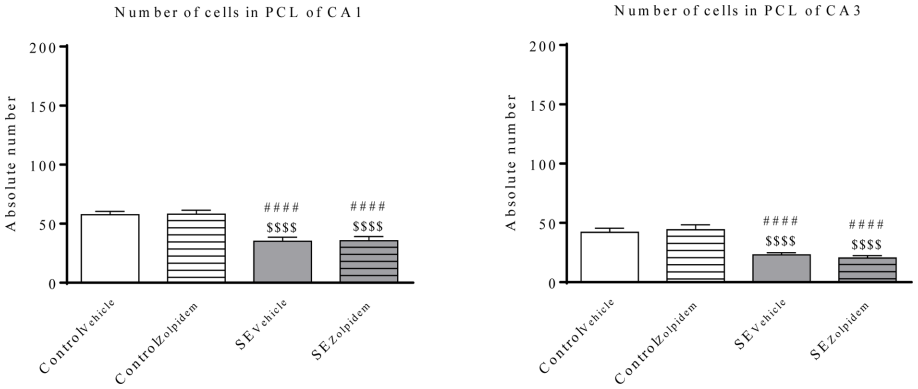

Fig. 4. Evaluation of absolute cell number (per 0.253 mm^2) in the PCL of the hippocampal CA1 in (A) $Control_{Vehicle}$, (B) $Control_{Zolpidem}$, (C) $SE_{Vehicle}$ and (D) $SE_{Zolpidem}$ (Left). One-way ANOVA was used to evaluate the absolute cell number of groups. Significant differences were annotated as follows: $^{\#\#\#\#}P<0.0001$ versus $Control_{Vehicle}$, $^{\$\$\$\$}P<0.0001$ versus $Control_{Zolpidem}$. Number of animals used for each group=4–6. Histological images are provided in Supplementary Data. Evaluation of absolute cell number (per 0.253 mm^2) in the PCL of the hippocampal CA3 in (A) $Control_{Vehicle}$, (B) $Control_{Zolpidem}$, (C) $SE_{Vehicle}$ and (D) $SE_{Zolpidem}$ (Right). One-way ANOVA was used to evaluate the absolute cell number of group ($Control_{Vehicle}$, $Control_{Zolpidem}$, $SE_{Vehicle}$, $SE_{Zolpidem}$). Significant differences were annotated as follows: $^{\#\#\#\#}P<0.0001$ versus $Control_{Vehicle}$, $^{\$\$\$\$}P<0.0001$ versus $Control_{Zolpidem}$. Number of animals used for each group=4–6. Histological images are provided in Supplementary Data.

comparison to $Control_{Vehicle}$ ($6.629 \times 10^7 \pm 2.936 \times 10^7$a. u., $P<0.001$). Furthermore, $SE_{Zolpidem}$ ($5.827 \times 10^7 \pm 2.062 \times 10^7$a. u.) was reported to exhibit significantly decreased NKCC1 expression compared to the $SE_{Vehicle}$ ($P<0.001$).

Discussion

Numerous studies have reported that zolpidem exerts a significant negative effect on memory in both humans and rats [39–41]. Consistent with our findings, zolpidem administration before the probe trial impairs memory retrieval in normal rats. Despite confirming the amnesic effect of zolpidem, these results contrast with those of studies showing that zolpidem does not cause memory

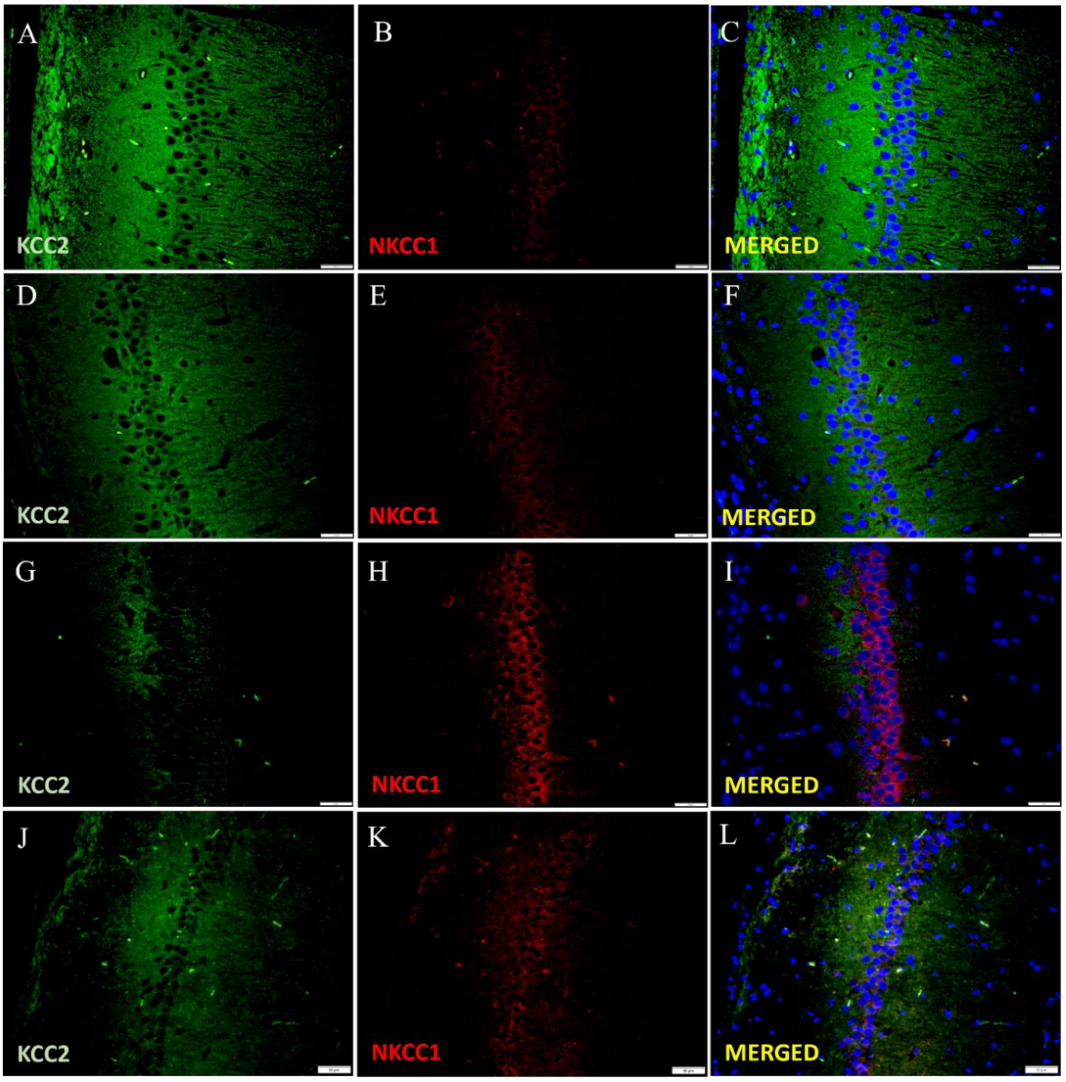

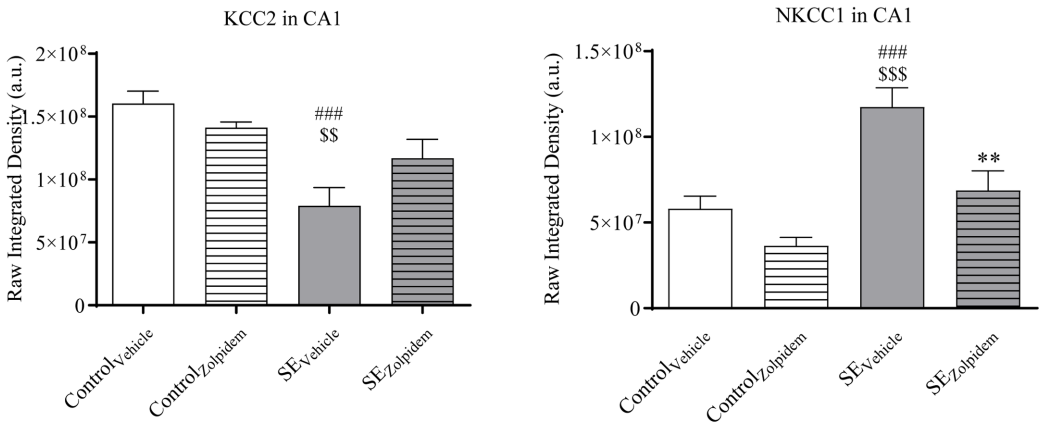

Fig. 5. Photomicrographs depicting fluorescence staining of KCC2 and NKCC1 in the hippocampal CA1 area (Top). Respective protein staining for each group was denoted as follow: (A-C) $Control_{Vehicle}$; (D-F) $Control_{Zolpidem}$; (G-I) $SE_{Vehicle}$; and (J-L) $SE_{Zolpidem}$. The scale bars represent 50 μm. Images were acquired at 400x magnification. Evaluation of the KCC2 and NKCC1 fluorescence intensity in the hippocampal CA1 area (Below). One-way ANOVA was used to evaluate the related intensity of groups. Significant differences were annotated as follows: $^{###}P<0.001$ versus $Control_{Vehicle}$ and $^{\$\$}P<0.01$ versus $Control_{Zolpidem}$ (KCC2); $^{###}P<0.001$ versus $Control_{Vehicle}$, $^{\$\$\$}P<0.001$ versus $Control_{Zolpidem}$ and $^{**}P<0.01$ versus $SE_{Vehicle}$ (NKCC1). Number of animals used for each group=4.

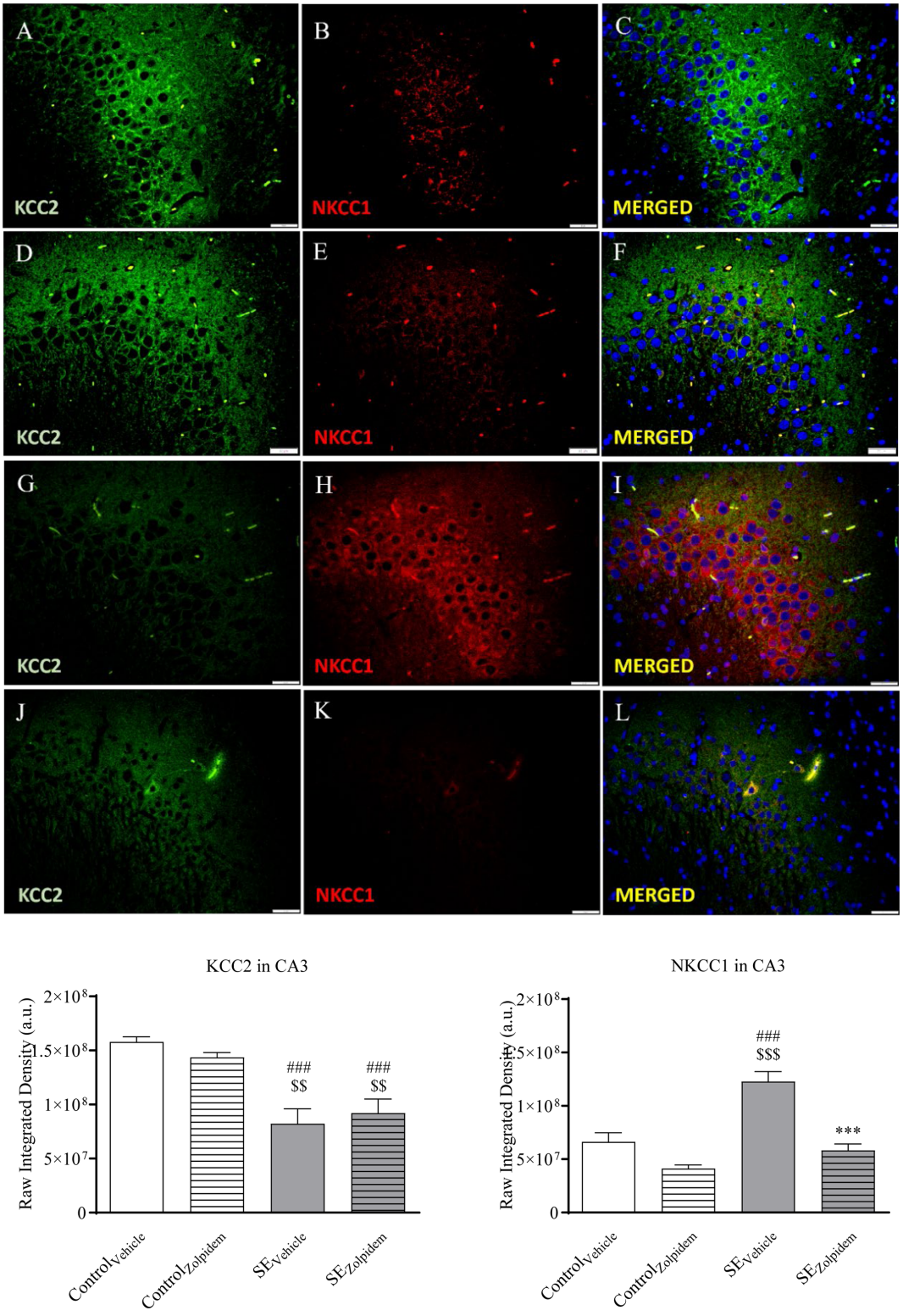

Fig. 6. Photomicrographs depicting fluorescence staining of KCC2 and NKCC1 in the hippocampal CA3 area (Top). Respective protein staining for each group was denoted as follow: (A-C) $Control_{Vehicle}$; (D-F) $Control_{Zolpidem}$; (G-I) $SE_{Vehicle}$; and (J-L) $SE_{Zolpidem}$. The scale bars represent 50 μm. Images were acquired at 400x magnification. Evaluation of the KCC2 and NKCC1 fluorescence intensity in the hippocampal CA3 area (Below). One-way ANOVA was used to evaluate the related intensity of groups. Significant differences were annotated as follows: $^{\#\#\#}P<0.001$ versus $Control_{Vehicle}$ and $^{\$\$}P<0.01$ versus $Control_{Zolpidem}$ (KCC2); $^{\#\#\#}P<0.001$ versus $Control_{Vehicle}$, $^{\$\$\$}P<0.001$ versus $Control_{Zolpidem}$ and $^{***}P<0.001$ versus $SE_{Vehicle}$ (NKCC1). Number of animals used for each group=4.

retrieval deficits [42, 43]. For example, [43] demonstrated that zolpidem did not impair memory retrieval in the plus maze discriminative avoidance task (PM-DAT). This inconsistency may be due to the different mechanisms by which zolpidem affects various aspects of memory. Similar to the MWM, the PM-DAT is also used to assess learning and memory; however, each task evaluates different memory aspects: the MWM assesses spatial memory (hippocampal-dependent), whereas the PM-DAT assesses fear- and anxiety-related learning and memory (hippocampal-independent). Based on our findings, we suggest that zolpidem is particularly selective or sensitive to the hippocampus and its functions. In SE rats, we found that zolpidem did not significantly affect memory retrieval, as it neither improved nor worsened impaired memory. Furthermore, acute zolpidem treatment in SE rats did not improve search strategy or swimming trajectory. This suggests that zolpidem-induced memory impairment is not evident under injury conditions, possibly due to the loss of function of the mechanisms that mediate the actions of zolpidem.

When assessing the effect of acute zolpidem administration on anxiety-like behavior, we found that zolpidem had an insignificant anxiolytic effect on normal rats. This is evident from the lack of reduction in path length in the pool periphery among zolpidem-treated animals. This minimal anxiolytic effect was also observed in the SE rats. Our findings align with those of previous research, suggesting that zolpidem exerts an insignificant anxiolytic effect in animals [43, 44]. Fear and anxiety are extensively linked to the GABAAR α2 subunit [45], to which zolpidem has a weak affinity [46]. This may explain the minimal anxiolytic effects of zolpidem observed in this study.

We also evaluated the effect of acute zolpidem administration on motor function by measuring swimming speed. This approach was used to assess motor function in the MWM task [29]. Zolpidem significantly impaired motor function in normal rats, supporting its sedative and hypnotic effects. Sedated animals exhibited impaired motor function, represented by a significant reduction in swimming speed. Our data is consistent with those of other studies showing that zolpidem significantly reduces motor activity due to its sedative/hypnotic effects on the α1-selective GABAAR subunit [46, 47]. The sedative effect of zolpidem was not observed in SE rats. This may be due to compromised mechanisms mediating the sedative/hypnotic effect in the SE condition, such as disruption of α1 subunit expression and its associated function.

SE mediated by pilocarpine has been associated with hippocampal injury and histopathology, particularly in the CA1 and CA3 subregions [48]. Consistently, we observed that both hippocampal regions in the $SE_{Vehicle}$ group exhibited a significant reduction in both cell layer thickness and absolute cell number compared to the $Control_{Vehicle}$ group. Disorganized cell layer architecture and condensed nuclear staining, reflected by the presence of pyknotic and apoptotic cells, particularly in the CA1 and CA3 subregions, further confirmed the significant extent of neuronal injury caused by SE. However, our study indicated that zolpidem does not exhibit a neuroprotective effect against neuronal death in SE-induced injury, as evidenced by the lack of significant differences in cell layer thickness and cell number. Thus, these results suggest that acute zolpidem may not mediate neuroprotection, at least in the hippocampus, following SE.

Next, we evaluated the potential effects of zolpidem on KCC2 and NKCC1 protein expression in the CA1 and CA3 subregions [48]. Pilocarpine-induced SE resulted in significant downregulation of hippocampal KCC2 expression compared to $Control_{Vehicle}$ animals. This confirmed the persistence of KCC2 downregulation in SE-induced neuronal injury, 24 days after SE induction. Our data also extend the findings of [49], who reported persistent hippocampal KCC2 downregulation 14 days post-SE induction. Additionally, KCC2 expression was significantly downregulated 45 days after SE induction [50]. Therefore, our findings, along with those of other studies, corroborate the long-term downregulation of KCC2 expression at various time points following SE induction.

Furthermore, our results revealed that zolpidem administration did not restore dysregulated KCC2 expression in hippocampal injury within the CA1 and CA3 subregions because KCC2 expression was indistinguishable between zolpidem-treated and vehicle-treated SE rats. Despite the insignificant upregulation in CA1 compared to that in vehicle-treated SE rats, we observed an increased pattern of KCC2 expression similar to that in control rats, which might indicate some level of restoration in this subregion. However, acute zolpidem administration may not be sufficient to upregulate or restore global hippocampal KCC2 expression to normal levels.

Previous studies have shown that chronic zolpidem administration significantly upregulated KCC2 expression in the limbic forebrain of normal mice [51]. Our findings on the potential involvement of zolpidem in mediating KCC2 upregulation align with those of [51]. However, our data showed a discrepancy in the changes in KCC2 expression following acute zolpidem treatment. These contrasting results may be due to the distinct cellular and functional conditions between the two studies

prior to zolpidem treatment. Zolpidem was administered to SE-injured animals, whereas [51] studied normal animals, which led to potentially incompatible cellular and physiological conditions.

Regarding NKCC1, we consistently observed long-term upregulation of NKCC1 in both hippocampal subregions of SE rats 24 days post-SE induction. This finding is consistent with that of [50], who reported sustained hippocampal NKCC1 upregulation 45 days post-SE induction [52]. A key finding of our study was that zolpidem consistently reduced or restored NKCC1 expression in rats, consistently across both hippocampal subregions. One potential mechanism is that zolpidem, acting as a positive allosteric modulator of GABAARs, could indirectly affect NKCC1 expression by modulating neuronal activity and restoring the balance between excitatory and inhibitory neurotransmission. As GABAAR activation typically leads to Cl^- influx, zolpidem may enhance inhibitory signaling, which could subsequently alter the homeostasis of ion transporters like NKCC1, involved in maintaining Cl^- gradients across neurons. Additionally, the modulation of GABAARs by zolpidem may trigger downstream signaling pathways that further influence NKCC1 expression. For example, alterations in intracellular Cl^- levels or changes in calcium signaling, both of which are influenced by GABAAR activity, could serve as signals for transcriptional or post-transcriptional regulation of NKCC1. Previous studies have shown that shifts in Cl^- gradients can impact the activity of ion transporters like NKCC1 and KCC2, which are critical for maintaining synaptic function and neuronal excitability as discussed in [53, 54]. Therefore, zolpidem's action on GABAARs may set off a cascade of intracellular events, ultimately modulating NKCC1 at the molecular level. These potential mechanisms warrant further investigation, as they could provide deeper insights into the broader role of GABAARs in regulating excitatory-inhibitory balance and ion transport in the brain. It is important to note that the role of GABAARs was not investigated in this study due to several significant limitations. First, the inclusion of diazepam in the treatment protocol, which also acts as a positive modulator of GABAARs, complicates the direct study of receptor blockade. Diazepam's mechanism of action enhances GABAergic signaling, making it difficult to isolate the effects of receptor inhibition without altering the overall treatment dynamics. Additionally, disrupting GABAergic inhibition during seizures potentially exacerbate seizure severity and increase neuronal damage. This potential risk, coupled with the challenges in isolating receptor-specific effects in the presence of diazepam, led us to decide against exploring GABAAR blockade in this study.

However, the zolpidem-mediated NKCC1 restoration in the hippocampus was not associated with improvements in learning or memory. This may be due to inadequate cellular recovery, in which proteins other than NKCC1 must be restored for behavioral enhancement. Alternatively, the restoration of NKCC1 alone, without concurrent KCC2 restoration, and possibly without restoration of Cl^- homeostasis, might underlie the lack of positive effects of zolpidem on behavioral impairments following neuronal injury. This assumption is supported by clinical studies reporting that patients with brain injuries who were previously prescribed zolpidem did not recover from behavioral impairments after zolpidem ingestion [55]. To date, no studies have specifically investigated the potential recovery effects of zolpidem on NKCC1 upregulation following neuronal injury. Several studies have reported significant reductions in NKCC1 upregulation in animal models of hypoxic ischemia, temporal lobe epilepsy, and traumatic brain injury following administration of vitexin, bumetanide, BDNF, and astaxanthin [49, 56, 57]. However, the mechanisms underlying the restorative effects of zolpidem on altered NKCC1 expression in neuronal injury remain unclear, and experimental evidence is lacking.

Therefore, further studies are required to elucidate the molecular mechanisms and downstream pathways through which zolpidem mediates NKCC1 downregulation in neuronal injury. Understanding these potential mechanisms, including the role of zolpidem in restoring NKCC1 expression or function and its indirect involvement in restoring Cl^- dysregulation, may help address the inconsistent clinical findings related to the paradoxical outcomes of zolpidem in neuronal injury.

Conclusion

Our *in vivo* study did not show any recovery of learning or memory after zolpidem administration in cases of brain injury. Additionally, acute zolpidem administration did not affect hippocampal pathology in brain injury, as these results were not comparable to those in vehicle-treated animals. Notably, acute zolpidem administration restored hippocampal NKCC1 expression, however, not KCC2 expression. From these observations, we can infer that the restoration of NKCC1 alone may not be sufficient to facilitate zolpidem-mediated recovery, particularly in learning and memory, under injurious conditions. Furthermore, our findings suggest that zolpidem has the potential to restore protein expression, at least in the hippocampus.

Acknowledgment

I would like to express my acknowledgement to the Ministry of Higher Education Malaysia for the funding under Fundamental Research Grant Scheme or FRGS (reference code: FRGS/1/2019/SKK10/USM/03/2). Not to forget, I am grateful to Associate Professor Dr Zurina Hassan from Centre for Drug Research, Universiti Sains Malaysia for providing facilities and guides for some parts of this study. Her support facilitated the smooth execution of the research.

References

1. Helmstaedter C. Cognitive outcome of status epilepticus in adults. Epilepsia. 2007; 48:(Suppl 8): 85–90. [Medline] [CrossRef]
2. Martinos MM, Yoong M, Patil S, Chong WK, Mardari R, Chin RF, et al. Early developmental outcomes in children following convulsive status epilepticus: a longitudinal study. Epilepsia. 2013; 54: 1012–1019. [Medline] [CrossRef]
3. Scott RC. What are the effects of prolonged seizures in the brain? Epileptic Disord. 2014; 16: S6–S11. [Medline] [CrossRef]
4. Lisman J, Buzsáki G, Eichenbaum H, Nadel L, Ranganath C, Redish AD. Viewpoints: how the hippocampus contributes to memory, navigation and cognition. Nat Neurosci. 2017; 20: 1434–1447. [Medline] [CrossRef]
5. Mutis JA, Rodríguez JH, Nava-Mesa MO. Rapidly progressive cognitive impairment with neuropsychiatric symptoms as the initial manifestation of status epilepticus. Epilepsy Behav Case Rep. 2016; 7: 20–23. [Medline] [CrossRef]
6. Danzer S. Mossy Fiber Sprouting in the Epileptic Brain: Taking on the Lernaean Hydra. Epilepsy Curr. 2017; 17: 50–51. [Medline] [CrossRef]
7. Cavarsan CF, Malheiros J, Hamani C, Najm I, Covolan L. Is Mossy Fiber Sprouting a Potential Therapeutic Target for Epilepsy? Front Neurol. 2018; 9: 1023. [Medline] [CrossRef]
8. Clauss RP, Güldenpfennig WM, Nel HW, Sathekge MM, Venkannagari RR. Extraordinary arousal from semi-comatose state on zolpidem. A case report. S Afr Med J. 2000; 90: 68–72. [Medline]
9. Arnts H, van Erp WS, Boon LI, Bosman CA, Admiraal MM, Schrantee A, et al. Awakening after a sleeping pill: Restoring functional brain networks after severe brain injury. Cortex. 2020; 132: 135–146. [Medline] [CrossRef]
10. Clauss R, Nel W. Drug induced arousal from the permanent vegetative state. NeuroRehabilitation. 2006; 21: 23–28. [Medline]
11. Kim C, Kwon BS, Nam KY, Park JW, Lee HJ. Zolpidem-Induced Arousal by Paradoxical GABAergic Stimulation: A Case Report With F-18 Flumazenil Positron Emission Tomography and Single Photon Emission Computed Tomography Study. Ann Rehabil Med. 2016; 40: 177–181. [Medline] [CrossRef]
12. Sutton JA, Clauss RP. A review of the evidence of zolpidem efficacy in neurological disability after brain damage due to stroke, trauma and hypoxia: A justification of further clinical trials. Brain Inj. 2017; 31: 1019–1027. [Medline] [CrossRef]
13. Hahm MH, Woo J. Paradoxical Motor and Cognitive Function Recovery in Response to Zolpidem in a Patient with Hypoxic-ischemic Brain Injury: A Case Report. Clin Psychopharmacol Neurosci. 2019; 17: 453–457. [Medline] [CrossRef]
14. Ben-Ari Y, Khalilov I, Kahle KT, Cherubini E. The GABA excitatory/inhibitory shift in brain maturation and neurological disorders. Neuroscientist. 2012; 18: 467–486. [Medline] [CrossRef]
15. Liu R, Wang J, Liang S, Zhang G, Yang X. Role of NKCC1 and KCC2 in Epilepsy: From Expression to Function. Front Neurol. 2020; 10: 1407. [Medline] [CrossRef]
16. Ben-Ari Y. Is the awakening produced by benzodiazepines due to excitatory actions of GABA? Transl Med Commun. 2021; 6: 1–6. [CrossRef]
17. Kurki SN, Uvarov P, Pospelov AS, Trontti K, Hübner AK, Srinivasan R, et al. Expression patterns of NKCC1 in neurons and non-neuronal cells during cortico-hippocampal development. Cereb Cortex. 2023; 33: 5906–5923. [Medline] [CrossRef]
18. Glien M, Brandt C, Potschka H, Voigt H, Ebert U, Löscher W. Repeated low-dose treatment of rats with pilocarpine: low mortality but high proportion of rats developing epilepsy. Epilepsy Res. 2001; 46: 111–119. [Medline] [CrossRef]
19. Hu K, Zhang C, Long L, Long X, Feng L, Li Y, et al. Expression profile of microRNAs in rat hippocampus following lithium-pilocarpine-induced status epilepticus. Neurosci Lett. 2011; 488: 252–257. [Medline] [CrossRef]
20. Brandt C, Töllner K, Klee R, Bröer S, Löscher W. Effective termination of status epilepticus by rational polypharmacy in the lithium-pilocarpine model in rats: Window of opportunity to prevent epilepsy and prediction of epilepsy by biomarkers. Neurobiol Dis. 2015; 75: 78–90. [Medline] [CrossRef]
21. Racine RJ. Modification of seizure activity by electrical stimulation. II. Motor seizure. Electroencephalogr Clin Neurophysiol. 1972; 32: 281–294. [Medline] [CrossRef]
22. Reddy DS, Kuruba R. Experimental models of status epilepticus and neuronal injury for evaluation of therapeutic interventions. Int J Mol Sci. 2013; 14: 18284–18318. [Medline] [CrossRef]
23. Modebadze T, Morgan NH, Pérès IA, Hadid RD, Amada N, Hill C, et al. A Low Mortality, High Morbidity Reduced Intensity Status Epilepticus (RISE) Model of Epilepsy and Epileptogenesis in the Rat. PLoS One. 2016; 11: e0147265. [Medline] [CrossRef]
24. Vorhees CV, Williams MT. Morris water maze: procedures for assessing spatial and related forms of learning and memory. Nat Protoc. 2006; 1: 848–858. [Medline] [CrossRef]
25. Vorhees CV, Williams MT. Assessing spatial learning and memory in rodents. ILAR J. 2014; 55: 310–332. [Medline] [CrossRef]
26. Timić T, Joksimović S, Milić M, Divljaković J, Batinić B, Savić MM. Midazolam impairs acquisition and retrieval, but not consolidation of reference memory in the Morris water maze. Behav Brain Res. 2013; 241: 198–205. [Medline] [CrossRef]
27. Wagner AK, Brayer SW, Hurwitz M, Niyonkuru C, Zou H, Failla M, et al. Non-spatial pre-training in the water maze as a clinically relevant model for evaluating learning and memory in experimental TBI. Neurobiol Learn Mem. 2013; 106: 71–86. [Medline] [CrossRef]
28. Higaki A, Mogi M, Iwanami J, Min LJ, Bai HY, Shan BS, et al. Recognition of early stage thigmotaxis in Morris water maze test with convolutional neural network. PLoS One. 2018; 13: e0197003. [Medline] [CrossRef]
29. Yang Y, Zhang M, Kang X, Jiang C, Zhang H, Wang P, et al. Thrombin-induced microglial activation impairs hippocampal neurogenesis and spatial memory ability in mice. Behav Brain Funct. 2015; 11: 30. [Medline] [CrossRef]
30. Harris RA, Lone A, Lim H, Martinez F, Frame AK, Scholl TJ, et al. Aerobic glycolysis is required for spatial memory acquisition but not memory retrieval in mice. eNeuro. 2019; 6: ENEURO.0389–18.2019. [Medline] [CrossRef]
31. Smolensky IV, Zubareva OE, Kalemenev SV, Lavrentyeva VV, Dyomina AV, Karepanov AA, et al. Impairments in cognitive functions and emotional and social behaviors in a rat lithium-pilocarpine model of temporal lobe epilepsy. Behav Brain Res. 2019; 372: 112044. [Medline] [CrossRef]

32. Perrault G, Morel E, Sanger DJ, Zivkovic B. Differences in pharmacological profiles of a new generation of benzodiazepine and non-benzodiazepine hypnotics. Eur J Pharmacol. 1990; 187: 487–494. [Medline] [CrossRef]
33. Griebel G, Perrault G, Letang V, Granger P, Avenet P, Schoemaker H, et al. New evidence that the pharmacological effects of benzodiazepine receptor ligands can be associated with activities at different BZ (omega) receptor subtypes. Psychopharmacology (Berl). 1999; 146: 205–213. [Medline] [CrossRef]
34. Paxinos G, Watson C. The rat brain in stereotaxic coordinates: hard cover edition. Elsevier. 2006.
35. He D, Chen H, Zeng M, Xia C, Wang J, Shen L, et al. Asthmatic Airway Vagal Hypertonia Involves Chloride Dyshomeostasis of Preganglionic Neurons in Rats. Front Neurosci. 2020; 14: 31. [Medline] [CrossRef]
36. Amaral DG, Scharfman HE, Lavenex P. The dentate gyrus: fundamental neuroanatomical organization (dentate gyrus for dummies). Prog Brain Res. 2007; 163: 3–22. [Medline] [CrossRef]
37. Makhlouf NA, El-Beshbishy RA, Abousetta A. Ginkgo modulates noise-induced hippocampal damage in male albino rats: a light and electron microscopic study. Egypt J Histol. 2014; 37: 159–174. [CrossRef]
38. François J, Germe K, Ferrandon A, Koning E, Nehlig A. Carisbamate has powerful disease-modifying effects in the lithium-pilocarpine model of temporal lobe epilepsy. Neuropharmacology. 2011; 61: 313–328. [Medline] [CrossRef]
39. Danjou P, Paty I, Fruncillo R, Worthington P, Unruh M, Cevallos W, et al. A comparison of the residual effects of zaleplon and zolpidem following administration 5 to 2 h before awakening. Br J Clin Pharmacol. 1999; 48: 367–374. [Medline] [CrossRef]
40. Otmani S, Demazières A, Staner C, Jacob N, Nir T, Zisapel N, et al. Effects of prolonged-release melatonin, zolpidem, and their combination on psychomotor functions, memory recall, and driving skills in healthy middle aged and elderly volunteers. Hum Psychopharmacol. 2008; 23: 693–705. [Medline] [CrossRef]
41. Huang MP, Radadia K, Macone BW, Auerbach SH, Datta S. Effects of eszopiclone and zolpidem on sleep-wake behavior, anxiety-like behavior and contextual memory in rats. Behav Brain Res. 2010; 210: 54–66. [Medline] [CrossRef]
42. Mikolajczak P, Okulicz-Kozaryn I, Szczawinska K, Kaminska E, Kus K. Zolpidem involvement on memory and hypnotic effect of ethanol in chronically ethanol-treated rats. Alcohol Alcohol. 1999; 34: 511–519. [Medline] [CrossRef]
43. Zanin KA, Patti CL, Sanday L, Fernandes-Santos L, Oliveira LC, Poyares D, et al. Effects of zolpidem on sedation, anxiety, and memory in the plus-maze discriminative avoidance task. Psychopharmacology (Berl). 2013; 226: 459–474. [Medline] [CrossRef]
44. Griebel G, Perrault G, Sanger DJ. Limited anxiolytic-like effects of non-benzodiazepine hypnotics in rodents. J Psychopharmacol. 1998; 12: 356–365. [Medline] [CrossRef]
45. Engin E, Benham RS, Rudolph U. An emerging circuit pharmacology of $GABA_A$ receptors. Trends Pharmacol Sci. 2018; 39: 710–732. [Medline] [CrossRef]
46. Crestani F, Martin JR, Möhler H, Rudolph U. Mechanism of action of the hypnotic zolpidem in vivo. Br J Pharmacol. 2000; 131: 1251–1254. [Medline] [CrossRef]
47. Rudolph U, Möhler H. GABAA receptor subtypes: Therapeutic potential in Down syndrome, affective disorders, schizophrenia, and autism. Annu Rev Pharmacol Toxicol. 2014; 54: 483–507. [Medline] [CrossRef]
48. Curia G, Longo D, Biagini G, Jones RS, Avoli M. The pilocarpine model of temporal lobe epilepsy. J Neurosci Methods. 2008; 172: 143–157. [Medline] [CrossRef]
49. Kourdougli N, Pellegrino C, Renko JM, Khirug S, Chazal G, Kukko-Lukjanov TK, et al. Depolarizing γ-aminobutyric acid contributes to glutamatergic network rewiring in epilepsy. Ann Neurol. 2017; 81: 251–265. [Medline] [CrossRef]
50. Li X, Zhou J, Chen Z, Chen S, Zhu F, Zhou L. Long-term expressional changes of Na+ -K+ -Cl- co-transporter 1 (NKCC1) and K+ -Cl- co-transporter 2 (KCC2) in CA1 region of hippocampus following lithium-pilocarpine induced status epilepticus (PISE). Brain Res. 2008; 1221: 141–146. [Medline] [CrossRef]
51. Shibasaki M, Masukawa D, Ishii K, Yamagishi Y, Mori T, Suzuki T. Involvement of the K+-Cl- co-transporter KCC2 in the sensitization to morphine-induced hyperlocomotion under chronic treatment with zolpidem in the mesolimbic system. J Neurochem. 2013; 125: 747–755. [Medline] [CrossRef]
52. Miller SM, Goasdoue K, Björkman ST. Neonatal seizures and disruption to neurotransmitter systems. Neural Regen Res. 2017; 12: 216–217. [Medline] [CrossRef]
53. Hartmann AM, Nothwang HG. NKCC1 and KCC2: Structural insights into phospho-regulation. Front Mol Neurosci. 2022; 15: 964488. [Medline] [CrossRef]
54. McMoneagle E, Zhou J, Zhang S, Huang W, Josiah SS, Ding K, et al. Neuronal K^+-Cl^- cotransporter KCC2 as a promising drug target for epilepsy treatment. Acta Pharmacol Sin. 2024; 45: 1–22. [Medline] [CrossRef]
55. Zhang B, O'Brien K, Won W, Li S. A retrospective analysis on clinical practice-based approaches using zolpidem and lorazepam in disorders of consciousness. Brain Sci. 2021; 11: 726. [Medline] [CrossRef]
56. Eftekhari S, Mehrabi S, Soleimani M, Hassanzadeh G, Shahrokhi A, Mostafavi H, et al. BDNF modifies hippocampal KCC2 and NKCC1 expression in a temporal lobe epilepsy model. Acta Neurobiol Exp (Warsz). 2014; 74: 276–287. [Medline] [CrossRef]
57. Zhang M, Cui Z, Cui H, Cao Y, Zhong C, Wang Y. Astaxanthin alleviates cerebral edema by modulating NKCC1 and AQP4 expression after traumatic brain injury in mice. BMC Neurosci. 2016; 17: 60. [Medline] [CrossRef]